Study of phase transitions in PNIPAm-Au photonic crystals

Dubinina Svetlana[1]

supervised by Dmitry Lapkin[2], Ivan Vartaniants[2, 3]

[1]*Moscow Institute of Physics and Technology, Moscow, Russia*

[2] *Deutsches Elektronen-Synchrotron DESY, Hamburg, Germany*

[3] *National Research Nuclear University MEPhI, Moscow, Russia*

Abstract

In situ X-ray diffraction studies of structural evolution of colloidal photonic crystals formed by gold spherical nanoparticles modified with poly-N-isopropylacrylamide (PNIPAm) upon incremental cooling and heating are reported. The Bragg peak parameters, such as peak position, integrated intensity, and radial and azimuthal widths and lattice parameter were analyzed as a function of temperature.

Contents

1. Introduction

Plasmonic nanoparticles have attracted significant interest as their spontaneous self-assembly can lead to the formation of periodic superstructures in which coupled plasmonic modes can be supported that are of interest for photonics, plasmonic lasing, and optoelectric devices. Today, thanks to advances in synthesis, the nanoparticles can be coated with different functional materials, such as metal nanoparticle cores with a hydrogel shell, that allow additional control over the plasmonic properties. The metal core can host the localized surface plasmon resonances while the hydrogel shell controls the inter-particle spacing to the visible wavelength range and can lead to plasmonic/diffractive coupling [1]. Moreover, the hydrogel shell can be functionalized to respond to different external stimuli, such as temperature, pH, or concentration gradients. Therefore, these core-shell particles are ideal building blocks for soft plasmonic superstructures with tailored optical properties, such as switchable photonic crystals.

While the hydrogel shell is responsible for interparticle interaction and promotes self-assembly of periodic structures, the metal core has the properties of localized plasmon resonances which could be beneficial not only for physics (photonics, different optoelectronic devices) but also for biology and medicine (PR is used for development of new type of sensors and types of diagnostics). The hydrogel shell is functionalized in such a way that it responds to raising and lowering of the temperature (Fig.1).

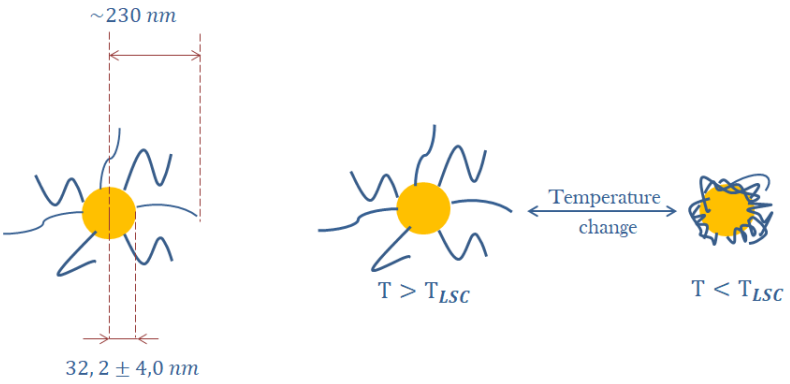

Figure 1. Scheme of PNIPAm-Au particle and its response on temperature change

As a result, the self-assembly of the PNIPAM colloids into crystal structures is completely controllable and switchable in-situ by temperature and has been extensively used to study phase transitions [2-4]. For the Au-PNIPAM colloids, it has already been shown that they allow the formation of highly ordered 2D plasmonic lattices that show surface lattice resonances as the result of plasmonic/diffractive coupling if the inter-particle spacing is on the order of the visible wavelength [5]. Their self-assembly into 3D crystals is expected to lead to novel photonic crystals with similar collective optical properties that can be controlled in-situ. Clearly, a complete understanding of the superlattice structure of the gold-cores is important for the controlled development of these novel materials.

2. Materials and methods

The core-shell particles studied in this work are gold nanoparticles modified with organic ligands poly-N-isopropylacrylamide. The size of the gold cores was estimated to be of 32.2 ± 4.0 nm from the TEM data (Fig. 2a,b). The position of the plasmon resonance peak in the UV-Vis spectrum (Fig. 2c) corresponds to the particle size of 32.5 nm.

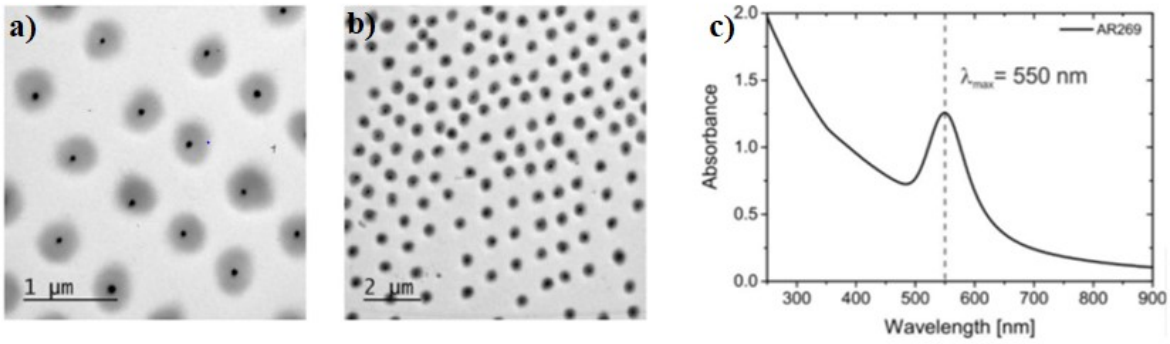

Figure 2. TEM image (a, b) and UV-vis spectrum (c) of PNIPAm-Au particles

To investigate the evolution of soft photonic crystal structure in response to temperature changes we performed an experiment at P10 Coherence Beamline at PETRA III using USAXS setup. The incident beam energy was 8.539 keV (0.145 nm), the beam size was 50×50 μm^2. Diffraction in transmission geometry was registered with Eiger 4M (2070×2167 px^2) detector which was located at a distance of 21,3 m from the sample.

The sample aqueous solution (12.7 wt) was sealed in a glass capillary. The capillary was fixed in a massive copper frame with a window to exclude temperature deviations. Heating and cooling of the sample were provided by coupled Peltier element and thermostat. The temperature of the sample was controlled by a thermocouple.

Series of diffraction patterns at different temperature values were recorded. Exposition time was set to 0.1 s to prevent the sample from radiation damage. Collected patterns were corrected in respect to the polarization of the incident beam.

a) 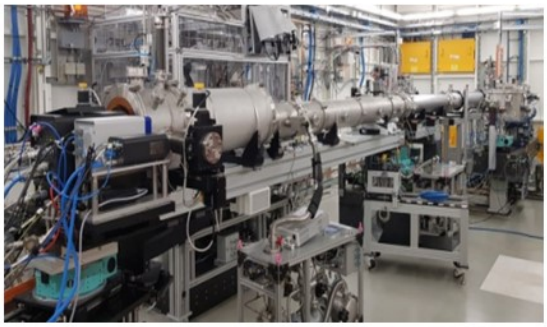 b) 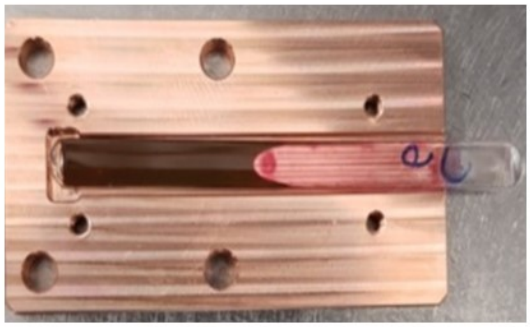

Figure 3. Experimental setup at P10 Coherent Beamline of PETRA III facility (a); a capillary with the sample solution in a copper sample holder (b)

To study evolution of Bragg peaks we fitted each of them with Gaussian and Lorentzian functions in two directions: radial (q_r) and azimuthal (q_φ):

$$f(x, I, q_0, w) = \frac{I * e^{-\frac{(x-q_0)^2}{2*w^2}}}{\sqrt{2\pi} * w} \quad - Gaussian\ function$$

$$f(x, I, q_0, w) = \frac{1}{\pi} * \frac{I*w}{(x-q_0)^2+w^2} \quad - Lorentzian\ function,$$

where I, q_0 and w were fitting parameters: I is the integral intensity, q_0 is the peak center position and $2 * w'$ for Lorenztian and $2 * w' * \sqrt{2 * ln2}$ for Gaussian function are the full width at half maximum (FWHM) values.

3. Results and Discussion

Here we thoroughly studied the crystallization of the PNIPAm-Au nanoparticles solution during cooling and the subsequent melting of the obtained crystal. Thus, two datasets were analysed. First dataset was obtained during cooling of the sample from 313 K down to 308 K and the second one was collected during heating of the sample from 308 K up to 317 K. The rate of temperature change was 0.1 K/min; diffraction patterns were collected every 30 sec. Evolution of the diffraction patterns with temperature for both datasets is shown in Figures 5 and 6, respectively.

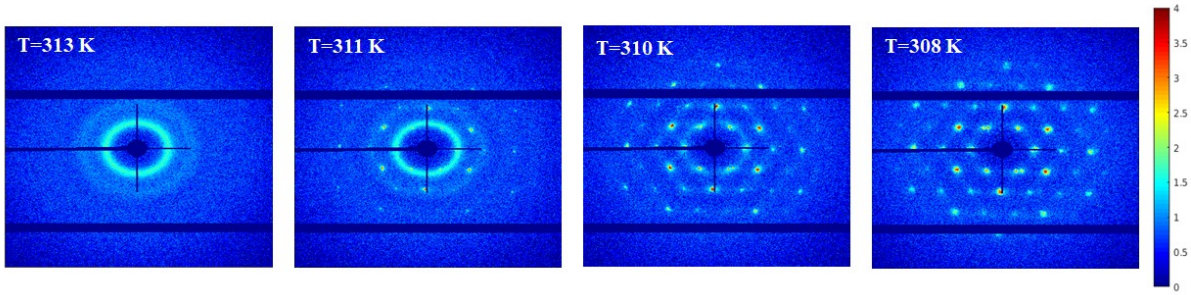

Figure 5. Examples of diffraction patterns collected at different temperatures during gradual cooling of PNIPAm-Au solution

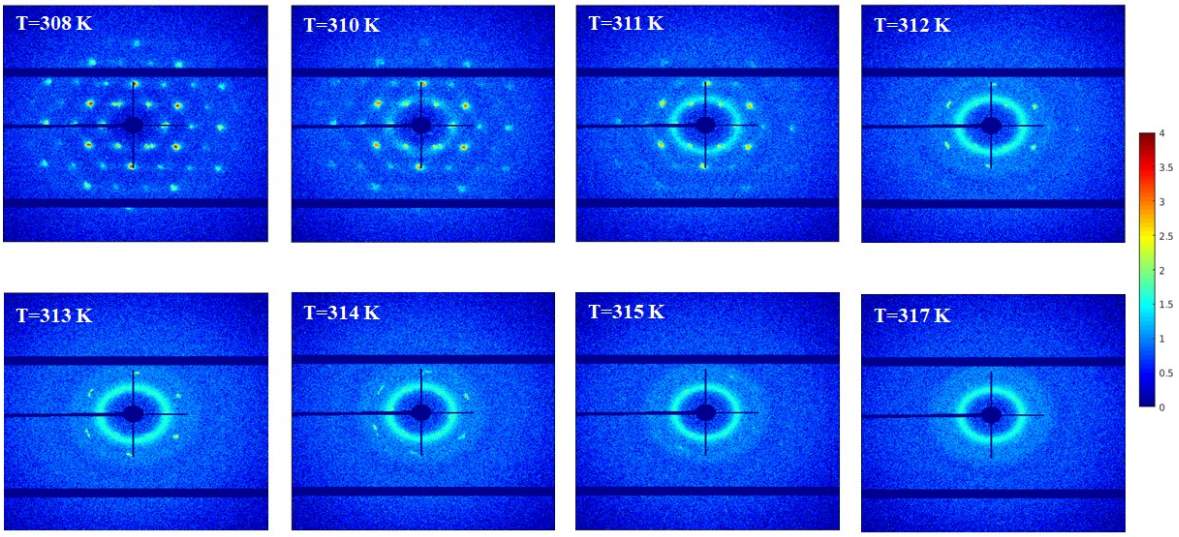

Figure 6. Examples of diffraction patterns collected at different temperatures during gradual heating of PNIPAm-Au solution.

Broad and isotropic rings on the pattern at the beginning of the cooling series are an evidence of the liquid state of the solution. The following appearance of Bragg peaks upon cooling indicates the sample crystallization. It is worth noting that there is a temperature range where the liquid rings coexist with the Bragg peaks, that means the sample crystallizes gradually.

On the contrary, the Bragg peaks disappear during heating and turn into amorphous rings as it is expected for the crystal melting.

The 6-fold symmetry of the patterns with Bragg peaks is a clear sign of a close-packing *hcp* structure (indexes of the peaks under assumption of the *hcp* structure are given in Fig. 7).

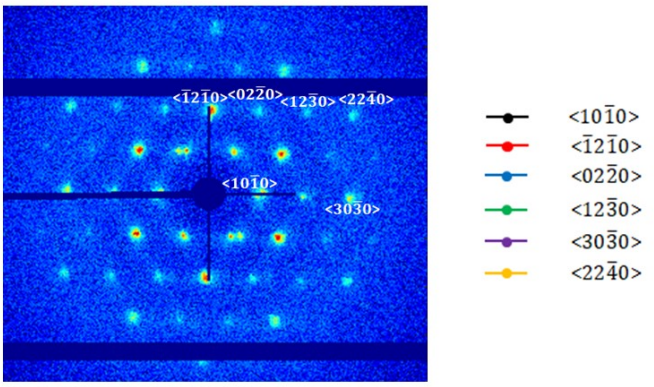

Figure 7. Designation of the diffraction pattern peaks assuming a close-packing hcp structure

3.1. Form factor and structure factor

The measured intensity is a product of two main factors: form factor of an Au particle and structure factor. The form factor is a footprint of the shape of the particles the sample consists of. The structure factor comprises information about the superlattice structure. In order to separate these two contributions, we analyzed the relatively wide-angle region of the patterns. Taking into account the size of the gold cores and the lattice periodicity, the intensity in this region is modulated mainly by the form factor. Assuming the particle shape to be spherical, the form factor is isotropic and can be described by the following equation:

$$P(q) = [\frac{1}{(qR)^3} * (\sin(qR) - qR * \cos(qR))]^2 \qquad (1)$$

As soon as it is isotropic, we analyzed angular-averaged radial intensity profiles. They were fitted with the spherical form factor given above in the q-region from 0.0069 to 0.0229 $Å^{-1}$. The form factor was calculated for a particle ensemble with normal distribution of the particle sizes. The mean particle diameter and its standard deviation were fitting parameters. Example of the radial intensity profile and the fit with spherical form factor are shown in Figure 8a. It was found, that the form factor corresponds to the particles with the size of 29.8 ± 4.0 nm and does not depend on the temperature. This value is in good agreement with the values obtained from the TEM and UV-Vis spectroscopy (see Materials and methods section).

Peaks at the small angles are conditioned by the structure factor. To extract the structure factor, the measured intensity was divided by the form factor. An example of the obtained structure factor (angular-averaged) is shown in Figure 8b.

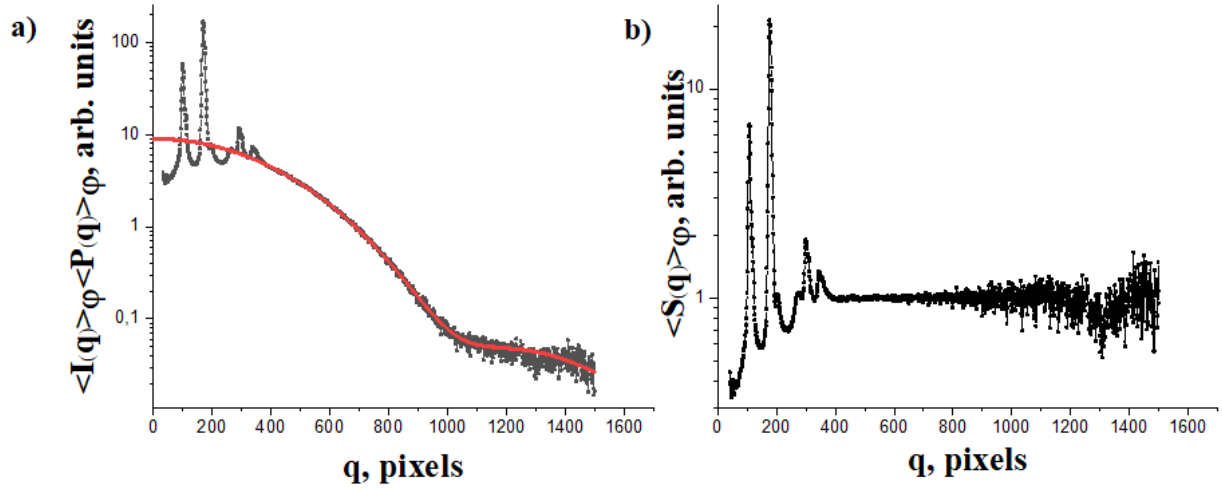

Figure 8. Radial intensity profile (angular-averaged) at 308 K (black dots and line) and its fit with the spherical form factor (red line) (a) and corresponding extracted structure factor (b)

From here on we will analyze only the obtained structure factor for each temperature. All data were converted into polar coordinates as it is shown in Figure 9a,b. To obtain statistically meaningful parameters of the Bragg peaks, we analyzed each peak in the ring separately and then calculated mean value and standard deviation. For each ring only a corresponding region of the diffraction pattern was analyzed (an example for the 1^{th} ring is shown in Figure 9c). The peaks were located analyzing mean profiles of the regions in two dimensions (shown in Figure 9d,f).

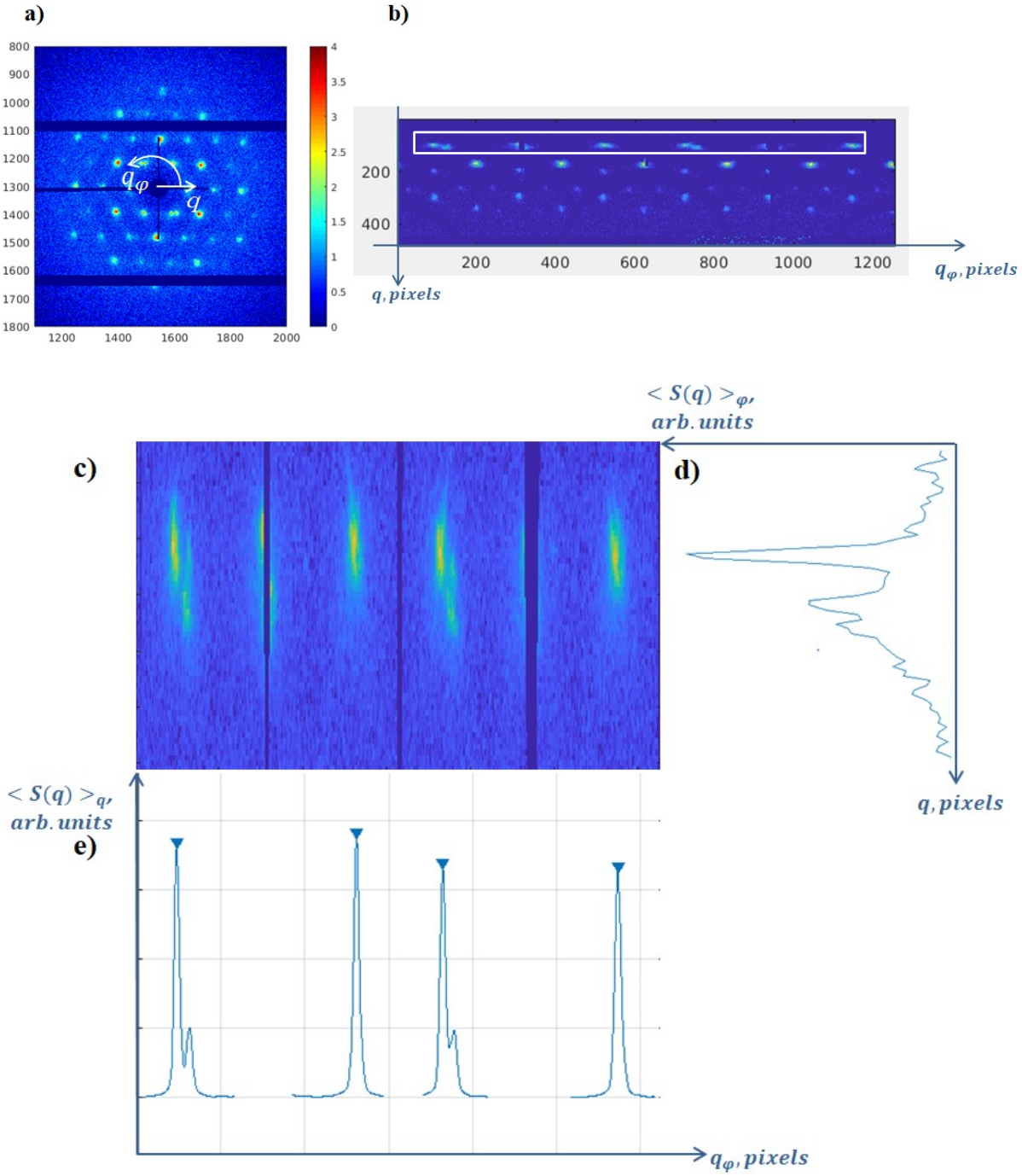

Figure 9. Diffraction pattern taken at 308 K (a); the same pattern after subtracting the form factor contribution in polar coordinates (b); the part of the pattern containing 1st ring (c) (also in the white frame in Figure 8b); the intensity distribution (structure factor) averaged in the angular direction for the 1st ring area (d); the intensity distribution (structure factor) averaged in the radial direction for the 1st ring area (e)

After the coordinates of the peaks were found, the intensity profiles taken in the corresponding positions were fitted by Gaussian and Lorentzian in two directions (Figure 10b,c) (as described in the Materials and methods section).

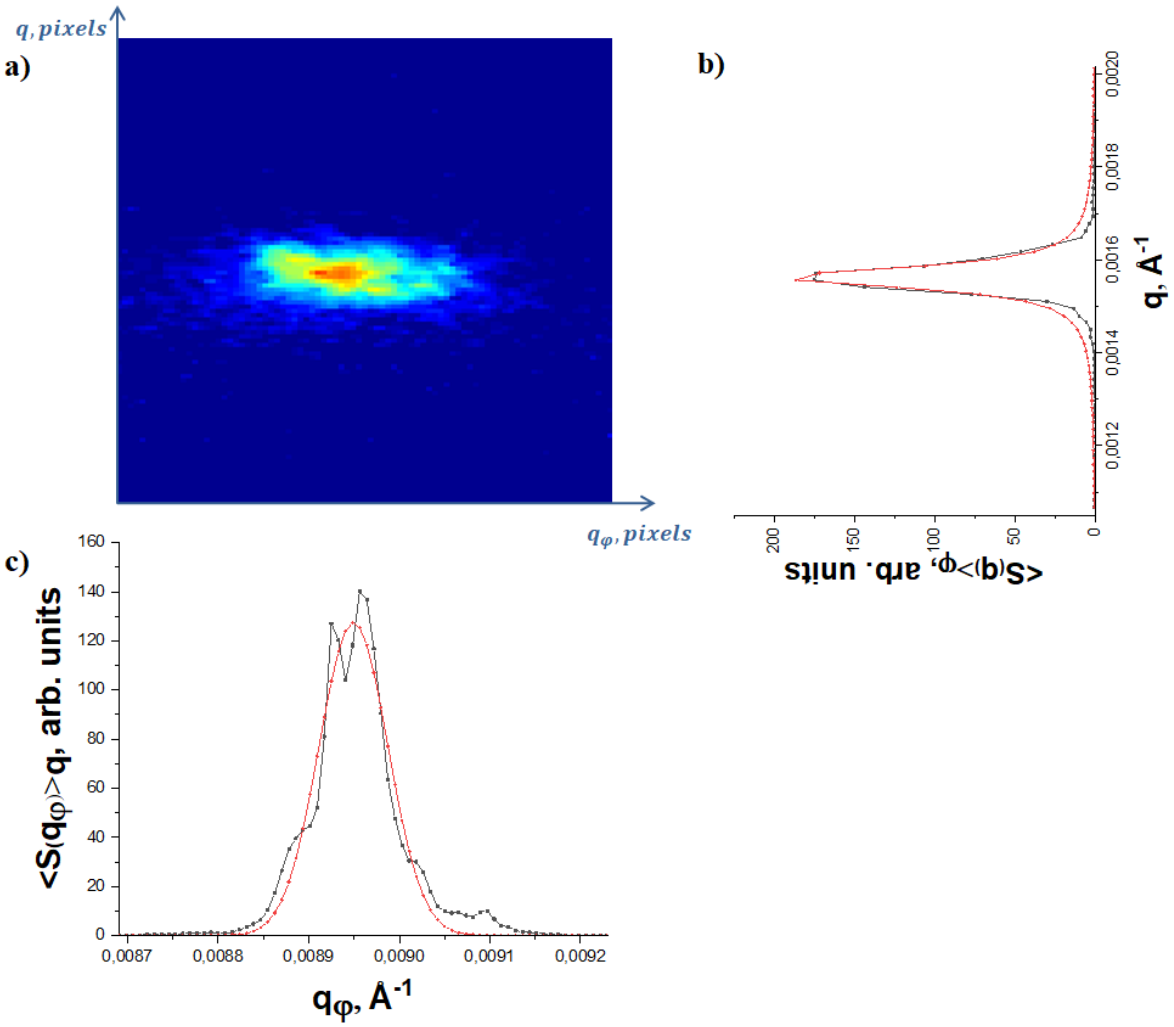

Figure 10. Examples of fitting for the 4th peak in the $10\bar{1}0$ ring (a), fitting was carried out in the radial (b) and angular(c) directions; black lines are experimental intensity distribution (structure factor), red lines are fitting with Lorentzian.

3.2. Temperature evolution of Bragg peak parameters

To investigate the structural evolution of PNIPAm-Au photonic crystals during cooling and heating, we performed a detailed analysis of the measured diffraction patterns shown in Figures 5 and 6. Based on the fact that the Lorentz function describes Bragg peaks with better accuracy, the following results are given based on

the data obtained as a result of the fit by Lorentzian. The values of each parameter were obtained by averaging this parameter over all peaks in the ring.

The following four parameters of the Bragg peaks as a function of temperature were analyzed: integrated intensity, Bragg peak position and full widths at half-maximum (FWHMs) in radial and azimuthal directions in reciprocal space.

Smooth transition from the liquid state to crystal form induces intensity changes. It can be seen from the figure (Fig. 11a) that with decreasing sample temperature the intensities of the Bragg peaks gradually grow. Fall of the intensity is observed during sample heating (Fig. 11b). This tendency points out to crystal melting. According to our results, a slow growth of the peak positions while sample was cooled can be observed (Fig. 11c). The results of the sample heating experiment indicate a gradual increase, and then slight decrease of the value of this parameter (Fig. 11d). The width of peaks in the radial direction as well as in the azimuthal direction increases with the increase of the temperature for the sample heating experiment (Fig. 11f,h). This indicates a crystals melting. Unexpected trends are observed in the evolution of the width of the Bragg peaks during the cooling experiment: with decreasing temperature, the peaks become wider for both directions (Fig. 11e,g). We consider that it could be connected with radiation damage.

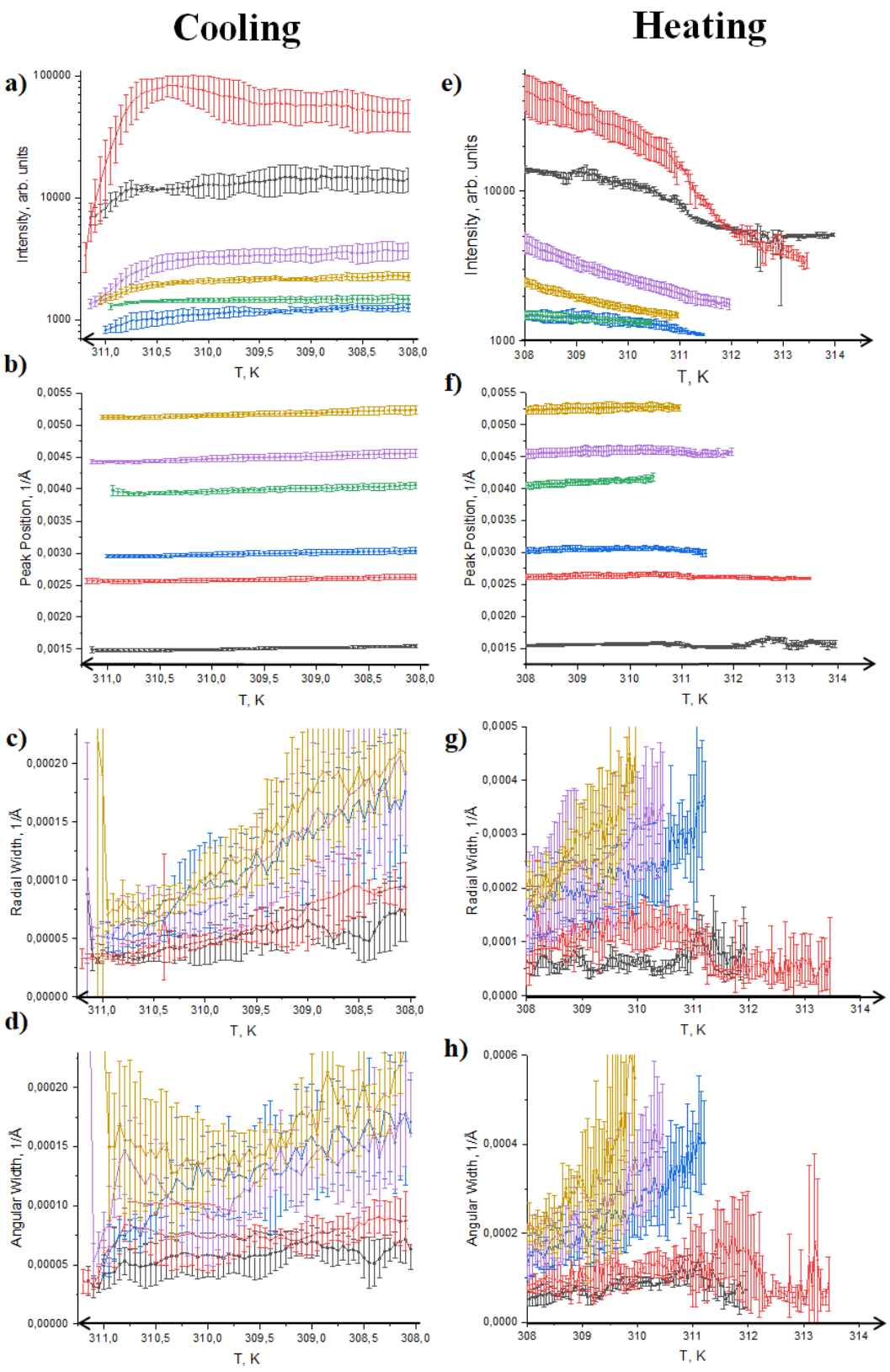

Figure 11. Temperature evolution of Bragg peak parameters during cooling (a,b,c,d) and heating (e,f,g,h) of the sample: intensity (a,e), peak position (b,f), FWHMs in radial (c,g) and azimuthal (d,h) directions. FWHM values are ommited for the $< 12\bar{3}0 >$ ring

Obtained peak positions were recalculated into the lattice parameter assuming the sample has an *hcp* structure. The lattice parameter as a function of temperature is shown in Figure 12.

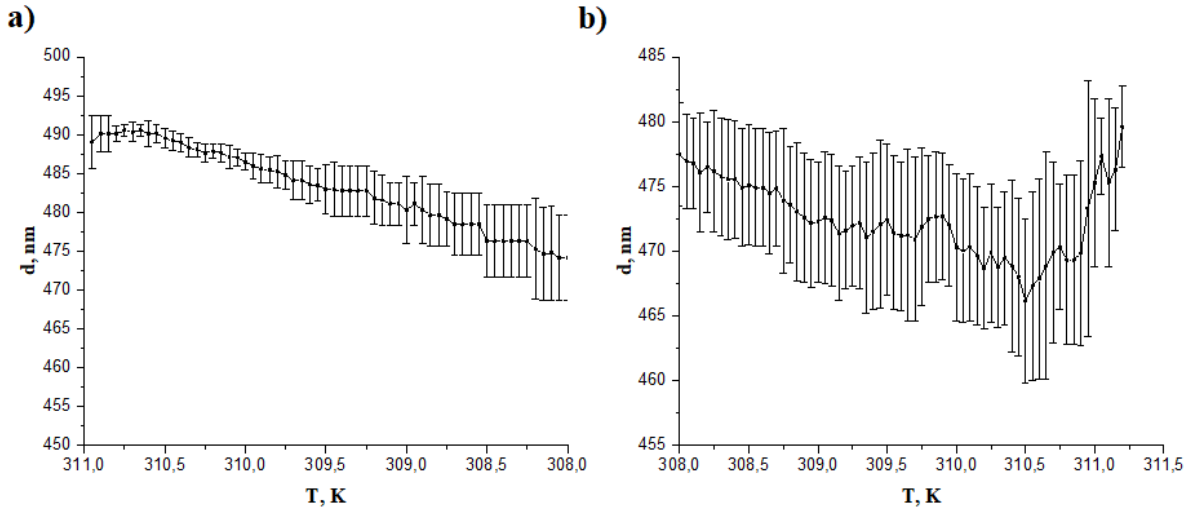

Figure 12. Temperature evolution of lattice parameter during the cooling (a) and heating (b) of the sample.

As it follows from our analysis, when the sample is cooled the lattice shrinks, which is associated with termal compression. In heating experiment the lattice shrinks gradually with increasing temperature from 308 to 310.5 K; but with subsequent heating it expands sharply.

4. Conclusion

In situ X-ray diffraction studies of structural evolution of colloidal photonic crystals at different temperatures were performed using the USAXS setup at the P10 beamline of the PETRA III synchrotron source. Photonic crystals formed by spherical gold nanoparticles modified with poly-N-isopropylacrylamide were investigated upon heating from 308 to 317 K and cooling from 313 to 308 K.

The structural changes in the colloidal crystal induced by sample heating and cooling were revealed by a detailed analysis of the measured Bragg peaks. The parameters of diffraction peaks, such as integrated intensities, the peak positions, and the peak widths in radial and azimuthal directions and also a lattice parameter were analysed as a function of temperature. The lattice parameter was shown to change with temperature.

Acknowledgments

The author is deeply grateful to her supervisor Dmitry Lapkin who has been the significant support throughout the entire project. I also express gratitude to Ivan Vartaniants for fruitful discussions and for the opportunity to work on this project. And I would like to thank the whole DESY summer school organization team.

References

1. M. Karg, et al., Adv. Funct. Mater., 21, 4668–4676 (2011) [DOI: 10.1002/adfm.201101115]

2. V.N. Manoharan, Science, 349, 1253751, (2015) [DOI: 10.1126/science.1253751]

3. M. Alsayed, et al. Science, 309, 1207-1210 (2005) [DOI: 10.1126/science.1112399]

4. Z. Wang, et al., Science, 338, 87-90 (2012) [DOI: 10.1126/science.1224763]

5. Volk, K.; et. al. Adv. Optical Mater. 2017, 5, 1600971, [DOI: 10.1002/adom.201600971]